[21] A. C. Templeton, S. Chen, S. M. Gross, R. W. Murray, *Langmuir* **1999**, *15*, 66 – 76.
[22] J. Liu, W. Ong, E. Román, M. J. Lynn, A. E. Kaifer, *Langmuir* **2000**, *16*, 3000 – 3002.
[23] C. S. Weisbecker, M. V. Merritt, G. M. Whitesides, *Langmuir* **1996**, *12*, 3763 – 3772.
[24] B. T. Houseman, M. Mrksich, *Angew. Chem.* **1999**, *111*, 876 – 880; *Angew. Chem. Int. Ed*. **1999**, *38*, 782 – 785.
[25] J. Jiménez-Barbero, E. Junquera, M. Martín-Pastor, S. Sharma, C. Vicent, S. Penadés, *J. Am. Chem. Soc*. **1995**, *117*, 11 198 – 11 204.
[26] J. C. Morales, D. Zurita, S. Penadés, *J. Org. Chem.* **1998**, *63*, 9212 – 9222.
[27] J. J. Distler, G. W. Jourdian, *J. Biol. Chem.* **1973**, *248*, 6772 – 6780.
[28] C. Tromas, J. Rojo, J. M. de la Fuente, A. G. Barrientos, R. Garciá, S. Penadés, unpublished results.
[29] H. H. Riese, A. Bernad, J. Rojo, A. G. Barrientos, J. M. de la Fuente, S. Penadés, unpublished results.
[30] The existence of this interaction has also been shown by using NMR spectroscopy: A. Geyer, C. Gege, R. R. Schmidt, *Angew. Chem.* **1999**, *111*, 1569 – 1571; *Angew. Chem. Int. Ed.* **1999**, *38*, 1466 – 1468.

Electronic Transduction of Polymerase or Reverse Transcriptase Induced Replication Processes on Surfaces: Highly Sensitive and Specific Detection of Viral Genomes**

Fernando Patolsky, Amir Lichtenstein, Moshe Kotler, and Itamar Willner*

Dedicated to Professor André M. Braun on the occasion of his 60th birthday

The detection of pathogens or autosomal recessive diseases is one of the future challenges of medicine and diagnostics.[1] Sensitive gene detection is accomplished by the polymerase chain reaction (PCR) amplification or secondary signal amplification routes.[2, 3] Major goals in future gene analysis include the parallel detection of a variety of pathogens and their quantitative assay. Inherent limitations of PCR prohibit the application of the method for quantitative and parallel high-throughput analyses. Microarrays of DNA have attracted substantial research efforts for the simultaneous analysis of genetic materials. In most of these systems the analyte samples are amplified by PCR cycles, and the microarrays act as a sensing interface that lacks amplification capabilities.[4, 5] Herein we address the development of ultrasensitive DNA-detection methods where in situ amplification proceeds on functionalized surfaces (electrodes or piezoelectric crystals) and the detection process is electronically transduced. The method enables the quantitative analysis of viral DNA and may be adopted for parallel analyses on arrays. Previous reports addressed the electrochemical[6–9] or microgravimetric,[10] quartz-crystal microbalance detection (QCM) of DNA. Several recent studies reported attempts to amplify DNA sensing processes: Dendritic, hyperbranched, oligonucleotides were employed to enhance the binding of DNA to electrodes.[11] The biocatalyzed precipitation of an insoluble product on the electronic transducer, that follows the primary hybridization between the analyte DNA and the probe oligonucleotide, was used to amplify the sensing event.[12] Also, labeled liposomes were employed as micromembrane interfaces that amplify the primary DNA-sensing events by their association to the probe-oligonucleotide/DNA-analyte complex generated on the transducer.[13, 14] Similarly, dendritic-type amplification of the analysis of a target DNA was accomplished by the use of oligonucleotide-functionalized Au-nanoparticles.[15] Faradaic impedance spectroscopy or frequency changes of the piezoelectric crystal, were used to transduce the different amplified sensing processes. Here we report a novel ultrasensitive method for the electronic transduction of the detection of viral nucleic acids. We demonstrate the surface polymerase-induced or reverse transcriptase stimulated formation of double-stranded DNA or RNA on the transducer, and the secondary amplification of the sensing process by the biocatalyzed precipitation of an insoluble product. Electrochemical and microgravimetric QCM methods are used as electronic transduction means for the DNA detection. The process is exemplified by the analysis of the M13 mp8 (M13ϕ) DNA (ca. 300 copies per 10 μL) and of the RNA of vesicular stomatitis virus (VSV; ca. 60 copies per 10 μL).

The method for analysis of the target is depicted in Scheme 1. The primer thiolated oligonucleotide **1**, complementary to a segment of the target M13 mp8 DNA, is assembled on an Au-electrode or an Au-quartz crystal through a thiol functional group.[16, 17] The sensing interface is then treated with the analyte DNA of M13 mp8 (+) strand, and the resulting complex on the transducer is treated with dATP, dGTP, dTTP, dCTP, and biotinylated-dCTP (ratio 1:1:1:2/3:1/3, nucleotides concentration of 1 mM) in the presence of DNA polymerase I, Klenow fragment (20 U mL^{-1}).[18] Polymerization and the formation of a double-stranded assembly with the target DNA is anticipated to provide the first amplification step of the analysis of the viral DNA. Polymerase introduces biotin tags to the double-stranded assembly, thus providing a high number of docking sites for the binding of the avidin – alkaline-phosphatase conjugate. The associated enzyme biocatalyzes the oxidative hydrolysis of 5-bromo-4-chloro-3-indolyl phosphate (**2**) to form the insoluble indigo product **3**, that precipitates on the transducer, thus providing a second amplification step for the analysis of the target DNA.[19] The synthesized strand on the electrode is anticipated to attract a positively charged redox label that can be assayed by chronocoulometry.[20] This approach enables us to monitor the polymerization process continuously. The negatively charged double-stranded assem-

[*] Prof. I. Willner, F. Patolsky, A. Lichtenstein
Institute of Chemistry
The Hebrew University of Jerusalem
Jerusalem 91904 (Israel)
Fax: (+972) 2-6527715
E-mail: willnea@vms.huji.ac.il
Prof. M. Kotler
Department of Experimental Pathology, The Hebrew University, Hadassah Medical School
Jerusalem 91120 (Israel)

[**] Parts of this research are supported by the Israel Ministry of Science as an Infrastructure Project in Biomicroelectronics and as an Israel – Japan cooperation. M.K. acknowledges the support of the American Foundation for Aids Research, AmfAR (grant No. 02730-28-RG).

  1433-7851/01/4012-2261 $ 17.50+.50/0

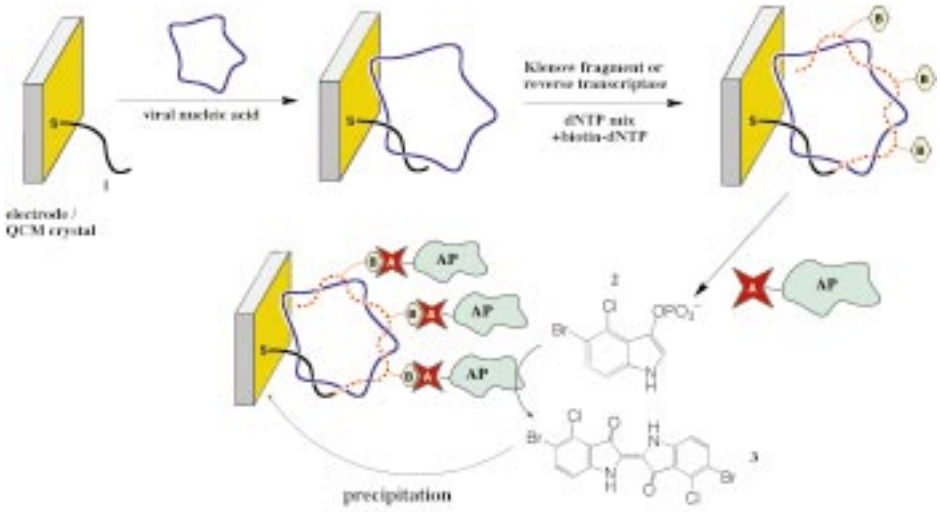

Scheme 1. Amplified electronic transduction of viral DNA/RNA by the polymerase-induced replication or reverse transcription and the biocatalyzed precipitation on an insoluble product of the transducer; AP = alkaline phosphatase, dNTP = mixture of dGTP, dATP, dTTP, and dCTP, broken red line = replicated nucleic acid, B in hexagon = biotin, A in red star = avidin.

bly is anticipated to repel a negatively charged redox probe, and to enhance the electron-transfer resistance on the transducer surface. The barrier for electron transfer to a negatively charged redox label in solution can be assayed by the Faradaic impedance spectroscopy technique.[21] Furthermore, hybridization, formation of the double-stranded assembly, polymerization, and precipitation of the insoluble product **3** alter the mass on the transducer. Thus, the entire set of detection steps of the target DNA may be assayed by microgravimetric analysis of the frequency change of a piezoelectric crystal.

The coverage of the probe oligonucleotide on the transducer was determined by microgravimetric QCM analysis and chronocoulometric experiments, using the $[Ru(NH_3)_6]^{3+}$ ion as redox label.[20] The surface coverage of the probe oligonucleotide on the transducer is controlled by the primer concentration and by the time of incubation of the transducer with the primer solution. Upon interaction of the Au-electrode with the primer **1**, 4.2×10^{-6} M, for 60 min, a surface with optimal surface coverage, corresponding to $6.3(\pm 0.3) \times 10^{-11}$ mol cm^{-2}, for the sensing of M13 ϕ was generated.

Figure 1 shows the chronocoulometric transients, in the presence of $[Ru(NH_3)_6]^{3+}$, of the probe-oligonucleotide-functionalized-electrode and of the sensing interface after hybridization with the analyte DNA. After 4 h hybridization, the charge associated with the linked redox probe was estimated to be 54 μC. Assuming that all of the $[Ru(NH_3)_6]^{3+}$ ions linked to the hybridized analyte DNA communicate electrically with the electrode, the surface covered by M13 mp8 DNA is about 9.0×10^{-13} mol cm^{-2}. Thus, only 1.5% of the sensing oligonucleotide units underwent hybridization with the viral DNA. This surface coverage of the hybridized DNA is supported by microgravimetric QCM measurements that reveal a frequency change of $\Delta f = -445$ Hz upon binding of the viral DNA to the surface. This frequency change translates to a surface coverage of the hybridized DNA of 1.1×10^{-13} mol cm^{-2}, which corresponds to hybridization to about 1.7% of the sensing interface.

The increase in the charge associated with $[Ru(NH_3)_6]^{3+}$ ions linked to the double-stranded assembly (Figure 2) is a result of the polymerase-induced formation of the double-stranded assembly with the analyte DNA which acts as template. The charge increases with time, implying that polymerization occurs on the surface, and levels-off after about 60 min of polymerization. Note that the charge associated with the analyte DNA is 29.2 μC, but the polymerization did not reach this value. Thus, the replication led only to 54% formation of the double-stranded assembly (on average

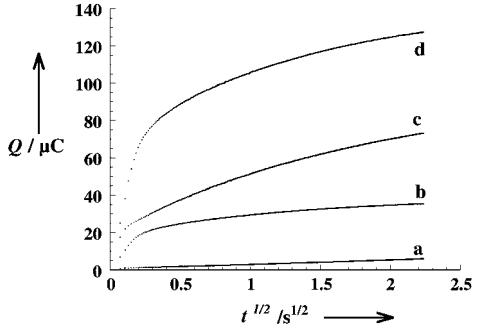

Figure 1. Chronocoulometric transients for: a) bare Au-electrode; b) **1**-modified Au-electrode; c) **1**-modified Au-electrode after hybridization with M13 ϕ (2.3×10^{-9} M) for 1.5 h, and d) after hybridization with M13 ϕ (2.3×10^{-9} M) for 4 h. All transients were recorded in the presence of $[Ru(NH_3)_6]^{3+}$, 5×10^{-5} M, in 10 mM Tris buffer, pH 7.4. The hybridizations were conducted in 0.1M phosphate buffer, pH 7.5, that included 30% formamide, at room temperature.

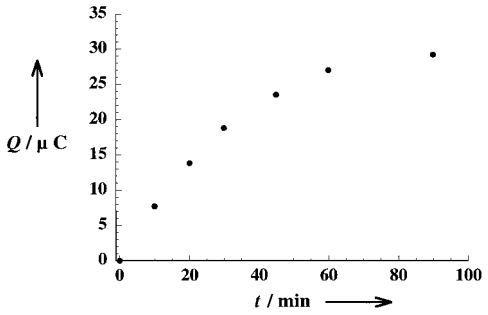

Figure 2. The time-dependent changes of the charge associated with the polymerase-induced polymerization and measured by chronocoulometry using $[Ru(NH_3)_6]^{3+}$ ions as the redox label in 10 mM Tris buffer, pH 7.4. The polymerization conditions are in ref. [18].

  1433-7851/01/4012-2262 $ 17.50+.50/0 *Angew. Chem. Int. Ed.* **2001**, *40*, No. 12

3900 bases were incorporated over each analyte DNA). This is attributed to steric constraints for the formation of the fully replicated double-stranded assembly on the surface or to the interruption of the Klenow fragment induced polymerization that is known to occur at specific sites during M13ϕ replication.[22] The partial polymerization on the surface is further reflected by QCM experiments that indicate that polymerization yields a frequency change of $\Delta f = -195$ Hz, whereas the attachment of the analyte DNA to the surface results in a frequency change of $\Delta f = -445$ Hz.

Figure 3 shows the Faradaic impedance spectra of the probe-oligonucleotide-functionalized electrode. The electron-transfer resistance R_{et} (diameter of the semicircle on the x axis)

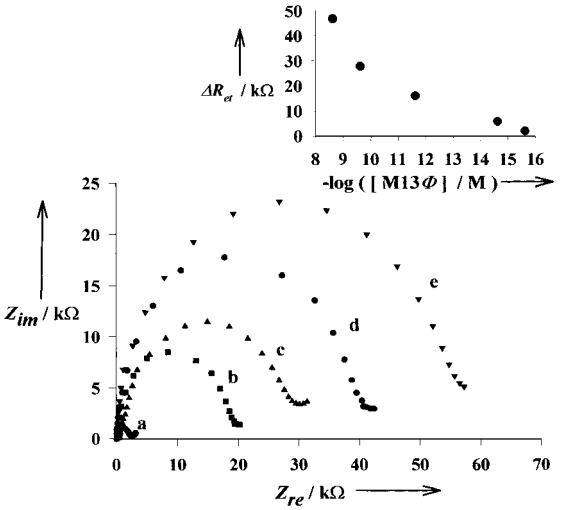

Figure 3. Faradaic impedance spectra (Nyquist plots) of: a) **1**-functionalized electrode; b) after hybridization with M13ϕ, 2.3×10^{-9} M; c) after the polymerase-induced replication and formation of the double-stranded assembly for 45 min; d) after the binding of the avidin–alkaline phosphatase conjugate to the surface; e) after the biocatalyzed precipitation of **3** for 20 min in the presence of **2** (2×10^{-3} M) in 0.1 M Tris buffer at pH 7.2. The hybridization and polymerization conditions are in the caption of Figure 1 and ref. [18]. Inset: The changes in the electron-transfer resistance ΔR_{et} upon the sensing of different concentrations of M13ϕ by the amplified biocatalyzed precipitation of **3** onto the electrode. The ΔR_{et} is the difference in R_{et} at the electrode after the precipitation of **3** for 20 min and R_{et} at the **1**-functionalized electrode.

increases upon the binding of the virus DNA from 3 kΩ to about 20 kΩ. This is consistent with the fact that binding of the high molecular weight DNA electrostatically repels the negatively charged redox label, $[Fe(CN)_6]^{3-}/[Fe(CN)_6]^{4-}$, from the electrode surface. The DNA polymerase-mediated synthesis of the complementary strand further increases the electron-transfer resistance to about $R_{et} = 33$ kΩ. Note that the polymerization does not double the interfacial electron-transfer resistance, consistent with the partial replication of the complementary strand on the target DNA molecule. The binding of the conjugate avidin–alkaline phosphatase and the subsequent biocatalyzed precipitation of **3** onto the electrode, results in an insulating layer that introduces a barrier for the interfacial electron transfer, and the R_{et} increases to $= 55$ kΩ. Similarly, microgravimetric QCM experiments reveal that at this concentration of the analyte DNA, the biocatalyzed precipitation of **3** on the crystal yields a decrease of $\Delta f = -1300$ Hz as a result of the mass increase on the transducer. The extent of the biocatalyzed precipitation of **3** on the transducers, and consequently the ΔR_{et} and Δf transduced signals, are controlled by the concentration of the M13 mp8 DNA in the sample, Figure 3 (inset) and Figure 4, respectively. Note that at concentrations of M13 mp8 corresponding to

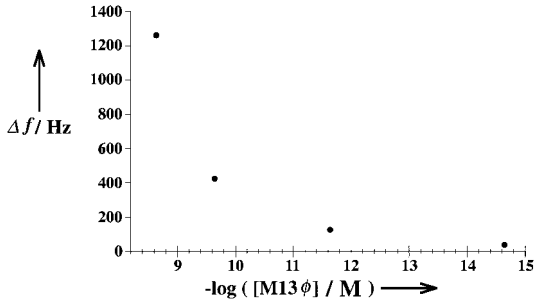

Figure 4. Frequency changes of the **1**-functionalized Au-quartz crystal upon the sensing of different concentrations of M13ϕ DNA as a result of the biocatalyzed precipitation of **3** onto the transducer. The conditions are in the caption of Figure 3.

2.3×10^{-15} M and 2.3×10^{-16} M, the hybridization of the analyte DNA with the sensing interface, and the subsequent polymerization, cannot be detected by Faradaic impedance spectroscopy or QCM, because of the low coverage of the hybridized analyte DNA on the respective transducers. In the electrochemical transduction, a change in the R_{et} of 2.8 kΩ is observed upon the analysis of the DNA, 2.3×10^{-16} M, as a result of the precipitation of **3**. In the microgravimetric analysis of the target DNA (2.3×10^{-15} M) a change of -36 Hz is observed as a result of the precipitation of **3** on the transducer.

A series of control experiments were performed to reveal the high specificity of the developed approach for sensing the targeted virus DNA: The foreign oligonucleotide **4** (see Scheme 1) that is not complementary to M13 mp8, was assembled on the electrode or Au-quartz crystal, but it failed to analyze the target DNA. Also, the **1**-functionalized electrode or QCM crystal were treated with denatured calf-thymus DNA (2.3×10^{-9} M) and the resulting transducers were subsequently subjected to polymerization, association of avidin–alkaline phosphatase, and the biocatalyzed precipitation of **3**. No binding of calf-thymus DNA with the sensing interfaces could be detected by impedance spectroscopy or QCM measurements. After the attempt to stimulate the biocatalyzed precipitation of **3**, a change of $\Delta f = -7$ Hz was observed, a value that may be considered as the noise level as a result of the nonspecific binding of avidin–alkaline phosphatase to the sensing interface. In another experiment the **1**-functionalized electrode or QCM crystal was treated with denatured calf-thymus DNA (2.3×10^{-9} M) mixed with an extremely low concentration (2.3×10^{-15} M) of M13ϕ DNA. The resulting assembly was subjected to polymerization and biocatalyzed precipitation. The observed change was $\Delta f = -31$ Hz, very close to the frequency change obtained with the target DNA only, implying that the sensing of M13ϕ is specific in the presence of DNA contaminants.

  1433-7851/01/4012-2263 $ 17.50+.50/0

A similar approach was used for the amplified sensing of the 11161 base RNA of vesicular stomatitis virus (VSV),[23] using reverse transcriptase as the replication biocatalyst.[24] The oligonucleotide **5** (see Scheme 1) was immobilized as the primer sensing interface on an Au-electrode or an Au-quartz crystal, surface coverage about 1.4×10^{-11} mol cm^{-2}.[16] Figure 5A shows the Faradaic impedance spectra of the **5**-functionalized electrode and the results observed upon the

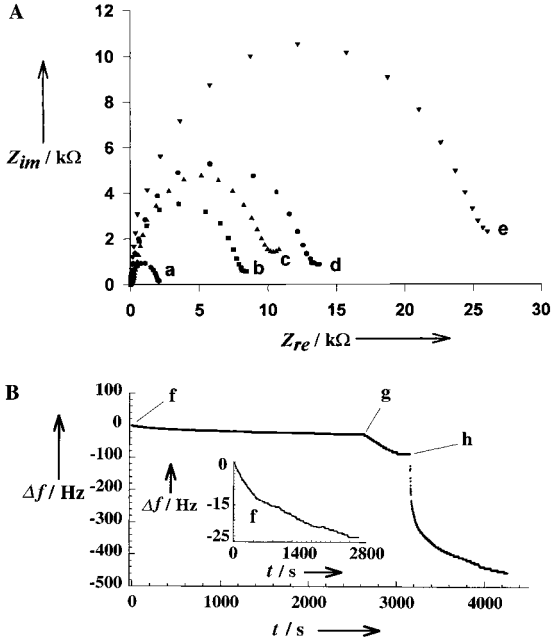

Figure 5. A) Faradaic impedance spectra (Nyquist plots) upon the amplified sensing of VSV RNA: a) the **5**-functionalized electrode; b) after hybridization with the VSV RNA, 1×10^{-12} M, in a solution consisting of 40 mM PIPES, 1 mM EDTA, 400 mM NaCl, 80% formamide, pH 7.5; c) after the reverse transcription for 45 min (80 U mL^{-1}) in the presence of dGTP, dATP, dTTP, dCTP, and biotinylated dCTP (1:1:2/3:1:1/3, each base 1 mM) in a solution consisting of 50 mM Tris buffer, 40 mM KCl, 8 mM $MgCl_2$, pH 8.3 at room temperature; d) after the association of the avidin–alkaline-phosphatase conjugate, bulk concentration 1 mM; e) after the biocatalyzed precipitation of **3** for 20 min in the presence of **2** (2×10^{-3} M) in Tris buffer pH 7.5. B) Time-dependent frequency changes of an Au-quartz crystal upon the analysis of the VSV RNA (1×10^{-12} M); f) frequency changes as a result of the replication of the bound RNA in the presence of reverse transcriptase and dGTP, dATP, dTTP, dCTP, and biotinylated-dCTP; g) upon the association of the avidin–alkaline-phosphatase conjugate; h) Upon the biocatalyzed precipitation of **3**. The conditions for the polymerization and biocatalyzed precipitation of **3** are detailed in Figure 5A. Inset: Magnification of curve f.

analysis of VSV–RNA according to the sequence outlined in Scheme 1. As expected, each of these steps increases the R_{et} at the electrode surface. For example, upon the analysis of 1×10^{-12} M VSV RNA the reverse transcription increases the interfacial R_{et} by $\Delta R_{et} = 4.5$ kΩ, the association of avidine–alkaline phosphatase further increases the R_{et} by 5.0 kΩ, and the precipitation of the insoluble product **3** onto the electrode increases the R_{et} by 14.0 kΩ. The viral RNA could be analyzed with a detection limit that corresponds to 1×10^{-17} M. At this concentration, the hybridization process and the reverse transcription of the VSV RNA were undetectable, yet the alkaline phosphatase precipitation of **3** onto the electrode resulted in an amplification path and the interfacial R_{et} increased by 2.2 kΩ. Control experiments revealed that the interaction of the sensing interface with a foreign RNA (1×10^{-9} M)[25] followed by an attempt to stimulate the reverse-transcription and the biocatalyzed precipitation of **3** resulted in a minute change in the R_{et} at the electrode ($\Delta R_{et} = 0.3$ kΩ) indicating that the amplified detection of the VSV–RNA is selective. Figure 5B shows the microgravimetric, QCM analysis of the RNA. Hybridization with the VSV–RNA, 1×10^{-12} M results in a decrease of $\Delta f = -72$ Hz that indicates a surface coverage of 1% of the sensing interface. The replication of the viral RNA in the presence of dGTP, dATP, dTTP, dCTP, and biotinylated-dCTP (1:1:1:2/3:1/3 base concentration 1 mM) in the presence of reverse transcriptase, 80 U mL^{-1}, results in a decrease of -26 Hz, Figure 5B, curve f. This frequency decrease translates to an average replication of the surface-associated analyte RNA of 36%. Binding of the avidin–alkaline phosphatase conjugate onto the surface is shown in curve g ($\Delta f = -52$ Hz) and the biocatalyzed precipitation of **3** results in a significant decrease in the crystal frequency that corresponds to around $\Delta f = 400$ Hz, curve h, Figure 5B.

In conclusion, we highlight novel methods for the rapid and sensitive electronic transduction of viral DNA/RNA by bioelectronic devices. These methods would find broad applicability in clinical diagnostics, environmental control, and food analysis. We have demonstrated highly sensitive detection methods for long nucleic acids, based on the polymerization or reverse transcription of the double-stranded assembly of the primers with the target viral DNA or RNA on surfaces, followed by the amplification of the sensing event by the biocatalyzed precipitation of an insoluble product on the transducer. Detection limits of 2.3×10^{-15} M and 2.3×10^{-16} M for the analysis of the virus-target DNA, were achieved by using microgravimetric and impedance transduction, respectively. The RNA detection limit was found to be 1×10^{-17} M (ca. 60 copies in 10 μL). This approach for the amplification of DNA/RNA sensing has broad and general potential applicability in biochip array technologies. By using redox-labeled nucleotides or fluorophore-labeled nucleotides as polymerization probes, amplified electrochemical or optical detection of viral DNA/RNA may be accomplished.

Received: December 11, 2000 [Z16253]

[1] a) I. M. Lubin, N. A. Yamada, R. M. Stansel, R. G. Pace, M. E. Rohlfs, L. M. Silverman, *Arch. Pathol. Lab. Med.* **1999**, *123*, 1177–1181; b) E. A. Winzeler, D. R. Richards, A. R. Conway, A. L. Goldstein, S. Kalman, M. J. McCullough, J. H. McCusker, D. A. Stevens, L. Wodicka, D. J. Lockhart, R. W. Davis, *Science* **1998**, *281*, 1194–1197; c) M. S. Yang, M. E. McGovern, M. Thompson, *Anal. Chim. Acta* **1997**, *346*, 259–275.
[2] a) U. Landegren, M. Nilsson, P. Y. Kwok, *Genome Res.* **1988**, *8*, 769–773; b) U. Landegren, *Curr. Opin. Biotechnol.* **1996**, *7*, 95–97.
[3] A. Isaksson, U. Landegren, *Curr. Opin. Biotechnol.* **1999**, *10*, 11–15.
[4] a) R. Ekins, F. W. Chu, *Trends Biotechnol.* **1999**, *17*, 217–218; b) G. H. W. Sanders, A. Manz, *Trends Anal. Chem.* **2000**, *19*, 364–378.
[5] a) D. Pinkel, R. Seagraves, D. Sudar, S. Clark, I. Poole, D. Kowbel, C. Collins, W. L. Kuo, C. Chen, Y. Zhai, S. H. Dairkee, B. M. Ljung, J. W. Gray, D. G. Albertson, *Nat. Genet.* **1998**, *20*, 207–211; b) D. T. Burke, M. A. Burns, C. Masterangelo, *Genome Res.* **1997**, *7*, 189–197.

  1433-7851/01/4012-2264 $ 17.50+.50/0

[6] T. de Lumley-Woodyear, C. N. Campbell, A. Heller, *J. Am. Chem. Soc.* **1996**, *118*, 5504 – 5505.
[7] K. M. Millan, A. Saraullo, S. R. Mikkelsen, *Anal. Chem.* **1994**, *66*, 2943 – 2948.
[8] S. Takenaka, K. Yamashita, M. Takagi, Y. Oto, H. Kondo, *Anal. Chem.* **2000**, *72*, 1334 – 1341.
[9] A. Bardea, F. Patolsky, A. Dagan, I. Willner, *Chem. Commun.* **1999**, 21 – 22.
[10] A. Bardea, A. Dagan, I. Ben-Dov, B. Amit, I. Willner, *Chem. Commun.* **1998**, 839 – 840.
[11] J. Wang, M. Jiang, T. W. Nielsen, R. C. Getts, *J. Am. Chem. Soc.* **1998**, *120*, 8281 – 8282.
[12] F. Patolsky, E. Katz, A. Bardea, I. Willner, *Langmuir* **1999**, *15*, 3703 – 3706.
[13] F. Patolsky, A. Lichtenstein, I. Willner, *J. Am. Chem. Soc.* **2000**, *122*, 418 – 419.
[14] F. Patolsky, A. Lichtenstein, I. Willner, *Angew. Chem.* **2000**, *112*, 970 – 973; *Angew. Chem. Int. Ed.* **2000**, *39*, 940 – 943.
[15] F. Patolsky, K. T. Ranjit, A. Lichtenstein, I. Willner, *Chem. Commun.* **2000**, 1025 – 1026.
[16] All primers were provided by Sigma-Genosys, UK. The primers were provided as disulfides, and the thiolated oligonucleotides were prepared by reacting the commercial disulfides with 0.04 M threo-1,4-dimercapto-2,3-butandiol (DTT) for 16 h at room temperature followed by the purification of the reduced DNA on a NAP-10 column (Pharmacia).
[17] Quartz crystals, 9 MHz AT-cut sandwiched between two Au-electrodes (area 0.196 cm^2, roughness factor ca. 3.5) were used in the studies.
[18] The M13 mp8 (+) strand, nucleotides, biotinylated-dCTP and Klenow fragment were all provided by Sigma. Polymerization was performed in a 10 mM Tris buffer solution, pH 7.5, that contained 50 mM of KCl, 5 mM $MgCl_2$, and 20 U mL^{-1} of the enzyme, dGTP, dATP, dTTP, dCTP, and biotinylated-dCTP (1:1:1:2/3:1/3, each base 1 mM).
[19] The avidin – alkaline phosphatase conjugate was coupled to the biotinylated surface by treating the electrodes or the quartz crystal with avidin – alkaline phosphatase conjugate (10 nmol mL^{-1}) in 0.1 M Tris buffer for 20 min. The resulting electrodes were treated with 2×10^{-3} M 5-bromo-4-chloro-3-indolyl phosphate (Aldrich) in a Tris buffer for 20 min.
[20] A. B. Steele, T. M. Hernland, M. Tarlov, *Anal. Chem.* **1998**, *70*, 4670 – 4677.
[21] A. J. Bard, L. R. Faulkner, *Electrochemical Methods: Fundamentals and Applications*, Wiley, New York, **1980**.
[22] L. Blanco, A. Bernard, J. M. Lazaro, G. Martin, C. Garmendia, M. Salas, *J. Biol. Chem.* **1989**, *264*, 8935 – 8940.
[23] HeLa cell cultures were inoculated with vesicular stomatitis virus-NJ. The culture medium was collected after 24 h, and clarified by centrifugation at 4 °C at 3000 g for 20 min. The supernatant solution was overlaid upon a 20% sucrose cushion in TNE buffer (TNE: 10 mM Tris buffer, pH 7.8, 100 mM NaCl, 1 mM EDTA; EDTA = ethylendiaminetetraacetate) and subject to centrifugation for 60 min at 27000 rpm with a SW 27 Beckmann ultracentrifuge. The pellet was dissolved in a mixture of 1:1 of phenol and TNE buffer that included 0.1% sodium dodecyl sulfate (SDS). Following extraction, the RNA was precipitated in ethanol that was incubated at −70 °C for 20 min and then subject to centrifugation for 20 min at 10000 rpm at 4 °C. The RNA was dissolved in TNE buffer.
[24] Enhanced avian reverse transcriptase product of Sigma.
[25] Yeast RNA of heterogeneous length of 2 – 7 kb (Boehringer Mannheim).

Cesium- and Rubidium-Selective Redox-Active Bis(calix[4]diquinone) Ionophores**

Philip R. A. Webber, George Z. Chen, Michael G. B. Drew, and Paul D. Beer*

The synthesis of redox-active molecular receptors designed to selectively recognize and electrochemically sense charged or neutral guest species of biological and environmental importance is an area of intense current interest.[1] A number of research groups have incorporated redox-active transition metal and organic centers into a variety of macrocyclic structural frameworks based on crown ethers, cryptands, and calixarenes, and shown some of these systems to be selective and electrochemically responsive to the binding of metal cations, particularly lithium,[2] sodium,[3] and potassium.[4] However, the construction of redox-active ionophores for the selective recognition of the larger cesium and rubidium metal cations has not, to our knowledge, been reported. This situation is surprising in view of the environmental concern for monitoring radioactive cesium in nuclear waste solutions[5] and the potential use of rubidium isotopes in radiopharmaceutical reagents.[6] We report here the synthesis, coordination, and electrochemical investigations of novel bis(calix[4]-diquinone) receptors L^1 and L^2, and demonstrate their remarkable ability to selectively complex and electrochemically sense cesium and rubidium cations.

Reaction of a solution of *p-tert*-butylcalix[4]arene (**1**) in acetonitrile with propane-1,3-ditosylate, 1,4-dibromobutane, or 1,5-dibromopentane in the presence of potassium carbonate gave the bis(calix[4]arene) derivatives **2**, **3**, and **4** in 30, 23, and 26% yields, respectively (Scheme 1). Oxidation of these compounds with $Tl(OCOCF_3)_3$ in trifluoroacetic acid[4a, 7] gave the new bis(calix[4]diquinone) ionophores L^1, L^2, and L^3 in respective yields of 28, 10, and 9% after column chromatography and recrystallization.[8]

Electrospray mass spectrometry (ES-MS) competition experiments gave the first qualitative indication that L^1 and L^2 displayed notable selectivity preferences for Cs^+ and Rb^+ ions. The electrospray mass spectra of equimolar Group 1 metal iodides in the presence of solutions of the tetraquinone ligands in DMSO revealed the most intense peaks occurred at

[*] Prof. P. D. Beer, P. R. A. Webber
Department of Chemistry
Inorganic Chemistry Laboratory, University of Oxford
South Parks Road, Oxford OX1 3QR (UK)
Fax (+44) 1865-272690
E-mail: paul.beer@chem.ox.ac.uk
Dr. G. Z. Chen
Department of Materials Science and Metallurgy
University of Cambridge
Pembroke Street, Cambridge CB2 3QZ (UK)
Prof. M. G. B. Drew
Department of Chemistry
University of Reading
Whiteknights, Reading RG6 2AD (UK)

[**] We thank the EPSRC for a studentship and the EPSRC and University of Reading for funds for the crystallographic image plate system.

Supporting information for this article is available on the WWW under http://www.angewandte.com or from the author.

  1433-7851/01/4012-2265 $ 17.50+.50/0